J. Phys. Chem. **1981**, *85*, 1874–1881

Decomposition of α-Aluminum Hydride Powder. 1. Thermal Decomposition

P. J. Herley,* O. Christofferson, and R. Irwin

Department of Materials Science and Engineering, State University of New York, Stony Brook, Long Island, New York 11794

(Received: September 12, 1980; In Final Form: January 28, 1981)

The thermal decomposition kinetics of α-AlH_3 powder have been determined between 130 and 150 °C. In this temperature range pristine and aged material, including powder which has been preirradiated with ^{60}Co γ-rays and high-intensity UV light, yielded sigmoidal fractional decomposition (α) vs. time curves. In all cases the $\alpha(t)$ curves exhibited three successive decomposition stages. The initial-period data for all materials can be described by a cubic expression representing rapid nucleation which is followed by a period of slow growth. Avrami–Erofeyev (A–E) kinetics accurately describe the data for the subsequent acceleratory and decay stages. Aging the material modifies the exponent of the A–E equation and is considered as a change from a three-dimensional random growth process to the two-dimensional random growth of a layered reaction/product interface. Similar activation energies were obtained for both processes. The increase in the specific rate constants which is induced by, and which is proportional to, the γ-ray and UV dose can be attributed to the presence of additional decomposition sites. These conclusions are consistent with independent scanning electron microscope observations of partially decomposed crystals. The same activation energy, 157.0 ± 12.5 kJ/mol, was obtained for both the acceleratory and decay periods of unirradiated and irradiated powder. The induction-period activation energy for all materials is 103.8 ± 11.0 kJ/mol. The rate constants increase with irradiation dose in a nonlinear manner. Irradiation also shortened the induction period (I). The I vs. total dose, Φ, data can be described by the equation $I = C_1 - C_2 \log \Phi$, a relationship derived from exponential nuclei growth during heating and linear nuclei growth during irradiation. Collectively these results indicate that the same decomposition process(es) occur in aged, pristine, and preirradiated powder. Irradiation increases the rate constants, and aging modifies the dimensionality of the A–E equation.

Introduction

This series of decomposition studies on α-aluminum hydride forms part of a program to obtain kinetic data on the decompositin of the covalent binary metal hydrides and the alkali and alkaline-earth alanates. These materials satisfy many of the requirements for use as hydrogen-storage materials and as light-weight, hydrogen-generating, solid propellants. To date, the materials reported on included $LiAlH_4$,[1,2] $NaAlH_4$,[3,4] and BaH_2, CaH_2, SrH_2, and MgH_2.[5]

The decomposition process in α-AlH_3 has been investigated isothermally, photolytically, and with simultaneous photolysis and thermal decomposition up to 150 °C. This paper will focus on the thermal aspects of the decomposition. The present study was preceded by a preliminary report[6] detailing part of the overall decomposition kinetics. Another brief earlier study[7] details the effects of UV irradiation on the subsequent thermal decomposition process, but the solvation state and the phase of the hydride were not reported. Also, we have carried out an electron microscope investigation[8] of the overall decomposition process concurrent with this work.

The earlier reports agree that the hydride decomposes isothermally according to the stoichiometry

$$2AlH_3 \rightarrow 2Al(s) + 3H_2(g)\uparrow$$

The reaction is irreversible and results in sigmoidal fractional decomposition, $\alpha(t)$, vs. time curves ($\alpha(t) = p/p_f$ where p is the measured pressure at time t, and p_f is the final pressure). An extensive literature exists[9,10] which relates the functional dependence of the various stages of the $\alpha(t)$ curves to the formation and growth of decomposition nuclei. We found that random nucleation and growth kinetics appeared to fit the data best. However, the Russian workers[7] reported a power-law α vs. t relationship with an arbitrarily defined induction period present up to $\alpha \simeq 0.2$. Specific details of the induction-period kinetics were not provided in either study.

Preexposure to ionizing radiation (γ-rays[6] or UV light[7] was found to accelerate the isothermal decomposition. However, details of the kinetics were not reported. Previous work on ammonium perchlorate,[11] lithium aluminum hydride,[1] and potassium permanganate[12] indicates that the isothermal decomposition kinetics can be affected markedly by prior exposure to ionizing radiation. In general the effects with increasing dose are a shortening of the induction period followed by an overall decrease in time required to complete the reaction. These effects have been interpreted as resulting from an increase in a critical parameter, e.g., the average "size" or concentration of the decomposition nuclei, with dose. A phenomenological relationship[13]

$$I = C_1 - C_2 \log \Phi \qquad (1)$$

---

[1] P. O. Herley and D. A. Schaeffer, *J. Phys. Chem.*, **82**, 155 (1978).

[2] P. J. Herley and D. H. Spencer, *J. Phys. Chem.*, **83**, 1701 (1979).

[3] D. Dougherty and P. J. Herley, *submitted to J. Phys. Chem.*

[4] J. W. Lauher, D. Dougherty, and P. J. Herley, *Acta Crystallogr., Sect. B*, **35**, 1454 (1979).

[5] D. Dougherty and P. J. Herley, *J. Less-Common Met.*, **73**, 97 (1980).

[6] P. J. Herley and R. H. Irwin, *J. Phys. Chem. Solids*, **39**, 1013 (1978).

[7] Yu. I. Mikhailov, Yu. G. Galitzyn, and V. V. Boldyrev, *Kinet. Katal.*, 17, 608 (1976). See also "The Control of the Reactivity of Solids", V. V. Boldyrev, M. Bulens, and B. Delmon, Eds., Elsevier, Amsterdam, 1979, p 48–51.

[8] P. J. Herley, O. Christofferson, and J. A. Todd, *J. Solid State Chem.*, **35**, 391 (1980).

[9] P. W. M. Jacobs and F. C. Tompkins, "Chemistry of the Solid State", W. E. Garner, Ed., Butterworths, London, 1955, Chapter 7.

[10] D. A. Young, "Decomposition of Solids", Pergamon, London, 1966.

[11] P. J. Herley and P. W. Levy, *J. Phys. Chem.*, **49**, 1493, 1500 (1968).

[12] E. G. Prout, *J. Inorg. Nucl. Chem.*, **1**, 368 (1958).

[13] P. W. Levy and P. J. Herley, *J. Phys. Chem.*, **75**, 192 (1971).

0022-3654/81/2085-1874$01.25/0

(C_1 and C_2 are constants) has been derived to explain the experimentally observed variation in the induction-period length, I, with irradiation dose, Φ, at constant temperature. This equation will be tested for α-AlH_3 powder in the present study.

The difference produced in the decomposition process between bulk ionization effects (caused by γ-rays) and effects occurring on or close to the surface (UV induced) is also of interest. The Russian workers reported that the power-law exponent in their kinetic equation fitted the data over the acceleratory period with values varying from 7 (for pristine material) to 1 for heavily UV-dosed material. Presumably these effects are limited to nuclei formation and growth on, and closest to, the exposed surfaces. The present study encompasses both ^{60}Co γ-ray-induced ionization events which occur principally within the solid and the UV-irradiation (surface) effects.

Experimental Section

Material. This work was facilitated by the availability of high-purity, single-phase, nonsolvated material.[14] The material was prepared by Dow Chemical Co. and is designated as pattern 1451. This material has been characterized crystallographically,[15] and its thermodynamic properties have been evaluated.[16] The space group was determined to be trigonal, $R\bar{3}c$, with six molecules in a hexagonal unit cell of dimensions $a = 4.449$ Å and $c = 11.804$ Å. This space-group assignment was confirmed from X-ray powder diffraction patterns using Cu Kα radiation.

The powder consists of uniform cuboid-shaped particles, 50–100 μm on a side. The crystallites were gray and were stored in the dark in a desiccator over anhydrous calcium sulfate (Drierite). The material was used without any further pretreatment. Care was taken to minimize exposure to the atmosphere during handling and weighing procedures, but, apart from excluding light, additional precautions were not observed in handling. A mass-spectrometric analysis of the as-received material indicated that detectable quantities of CO_2, N_2, and O_2 were evolved just before the evolution of H_2 at a heating rate of 30 °C/min. The weight percent of carbon in the sample was determined to be 0.23% by using standard carbon combustion techniques. Gas chromatography indicates the presence of two impurity peaks, each corresponding to ~200 ppm of organic solvent contaminant. The precentage decomposition of a typical sample after heating to $\alpha = 1$ at 130 °C was found to be 97.0%, determined by weight-loss measurements using a Perkin-Elmer AM-1 Autobalance.

Procedure. Samples weighing 3.0–60.0 mg were contained in a platinum boat and decomposed isothermally in a conventional constant-volume, Pyrex-glass, high-vacuum system with liquid-nitrogen traps. The decomposition chamber and the furnace were similar to the apparatus described previously.[11] The pressure data were recorded on a Hewlett Packard digital recorder, Model 5055A, every 60 s. In the subsequent figures the data presented as symbols are typical points on virtually continuous curves. The nonlinear, least-squares, curve-fitting program was done on a UNIVAC 1100 computer using a system library program utilizing Marquardt's method.[17]

For γ irradiation the material was encapsulated in baked fused-silica ampules, sealed under vacuum, and wrapped light-tight in aluminum foil. The samples were irradiated at ambient temperature with ^{60}Co γ-rays from the spent-fuel facility at Brookhaven National Laboratory. The γ-ray dose rate varied between 5.5×10^4 and 5.3×10^6 R/h. For a fixed dose, over this dose range, it was found that the results were dose-rate independent; i.e., a variation in the dose rates produced no perturbation on the subsequent irradiation effect provided the same total dose was administered. For UV photolysis the samples were exposed to UV light from a 1000-W BH6 lamp for a fixed time and at a predetermined lamp intensity.

Results

These kinetic studies can be grouped under two principal headings: pristine material and preirradiated material. Decomposition of pristine material focuses on the basic kinetics of the decomposition process. This is influenced by intrinsic defects in the material and includes the effects of aging. Preirradiation induces additional defects into the crystal which modify the α vs. time curves during the subsequent thermal decomposition. The following subsections contain the relevant data.

Pristine Material. The isothermal decomposition of 3 mg of pristine powder produces sigmoid α vs. t curves in the temperature range 100–150 °C (Figure 1). The day-to-day reproducibility of the runs is satisfactory; e.g., three successive runs at 130 °C are included in Figure 1. However, this reproducibility does not persist over extended storage periods. Aging of the material occurs at room temperature under normal laboratory conditions, but it is extremely slow. For example, no detectable change was produced in the α vs. t curves after the cuboids were exposed to air for 3 weeks at room temperature. However, an identical decomposition run on material stored in the dark for 18 months resulted in a faster decomposition. All stages of the $\alpha(t)$ vs. time curve were affected to the same degree. The quantity of gas evolved in both runs did not differ significantly. Presumably the aging process involves very slow decomposition at room temperature. Electron microscope evidence supports this contention; some decomposition nuclei have been observed in the solid prior to decomposition. Also, the gray appearance of the powder (it was reportedly white on synthesis[14,15]) is further evidence that decomposition is occurring. Moreover, the material is photosensitive to UV light at room temperature, and prior handling procedures may have resulted in the material receiving an exposure.

This aging effect notwithstanding, the material is remarkably inert as the following attempts to explore its chemical reactivity will show. The decomposition was carried out with the powder intimately admixed with various solids: (i) its own finely divided final product; (ii) finely divided 99.999% pure Al powder (43-μm particle size); (iii) fused silica powder; and (iv) alumina powder in proportions ranging from 1:1 to 1:10 (AlH_3/solid). These mixtures produced no change on the subsequent thermal decomposition at 140 °C. Exposure to a saturated water-vapor atmosphere from 2-min to 1-week periods produced no effect on the subsequent α vs. time curves; after 14-days exposure the hydrogen gas evolution at 140 °C appeared to take slightly longer (~10 min), but the curves were the same shape and the same volume of gas

---

(14) F. M. Brower, W. E. Matzek, P. F. Reigler, H. W. Rinn, C. B. Roberts, D. L. Schmidt, J. A. Snover, and K. Terada, *J. Am. Chem. Soc.*, **98**, 2450 (1976).

(15) J. W. Turley and H. W. Rinn, *Inorg. Chem.*, **8**, 18 (1969).

(16) G. C. Sinke, L. C. Walker, F. L. Oetting, and D. R. Stull, *J. Chem. Phys.*, **47**, 2759 (1967).

(17) D. W. Marquardt, *J. Soc. Ind. Appl. Math.*, **11**, 431 (1963); D. A. Meeter, nonlinear least-squares program GAUSHAUS, University of Wisconsin Computing Center, 1964; program revised 1966.

(18) M. Avrami, *J. Chem. Phys.*, **9**, 177 (1941); B. V. Erofeyev, *C. R. Acad. Sci. Russ.*, **52**, 511 (1946).

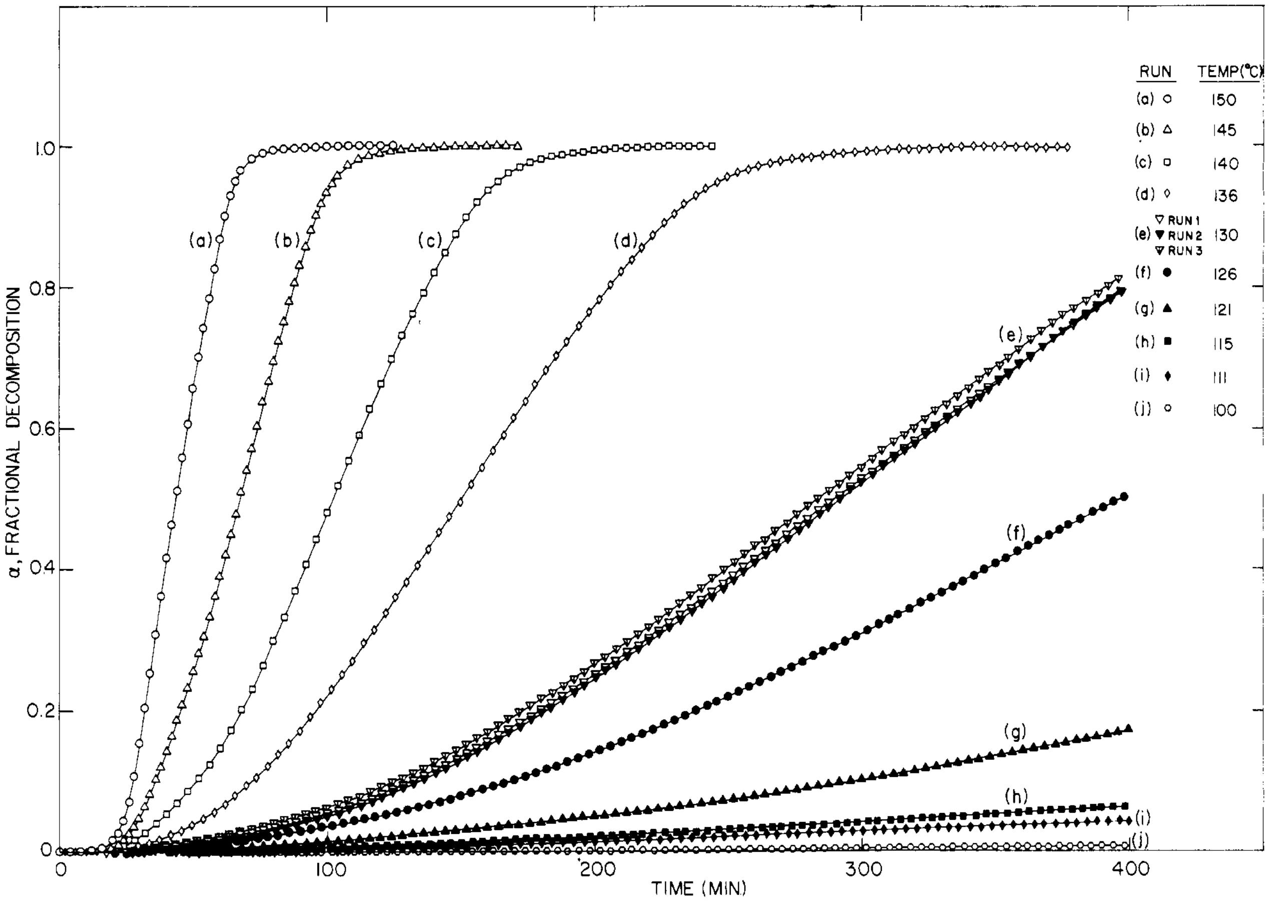

Figure 1. Effect of temperature on the isothermal decomposition of α-AlH_3 powder in vacuo. The plot shows the fractional decomposition, $\alpha = p(t)/p_f$, vs. time curves for gas evolution from 60 mg of α-AlH_3 powder between 100 and 150 °C. Also included are three runs at 130 °C to indicate typical reproducibility of the data.

(identical sample weight) was evolved, within experimental error (±1%).

Since the kinetics reported previously do not agree, the $\alpha(t)$ vs. time data were carefully analyzed. All of the curves can be resolved into three distinct stages: an initial induction period up to $\alpha \approx 0.04$[6] followed by an acceleratory stage ($0.06 < \alpha < 0.6$) which terminates in a decay period. Several kinetic equations[9] were applied to the data; however, for various reasons, only te Avrami–Erofeyev[7] (A–E) equation proved suitable for fitting the acceleratory- and decay-period data consistently over large time frames and the entire temperature regime with satisfactory correlation coefficients (Figure 2). The A–E equation was applied in the form

$$[-\ln (1 - \alpha)]^{1/n} = kt + \text{constant} \qquad (2)$$

where $n = 2$ and $k = k_2$ for the acceleratory period, and $n = 3$ and $k = k_3$ for the decay period. Before the 18-month aging period, A–E kinetics were also applicable to the α vs. time data but with $n = 4$ over the acceleratory period and $n = 3$ over the decay stage. The change in the value of the exponent and an increase in the overall rate are the only significant changes which were found in the decomposition kinetics after 18 months.

The induction-period data proved to be the most difficult to fit satisfactorily. They could only be fitted adequately by the power law

$$\alpha^{1/3} = k_1 t + \text{constant} \qquad (3)$$

and partially by the same equation with the exponent = 1/2. The latter form was rejected on the basis that the extent of fit ($0.001 < \alpha < 0.01$) was smaller than that for

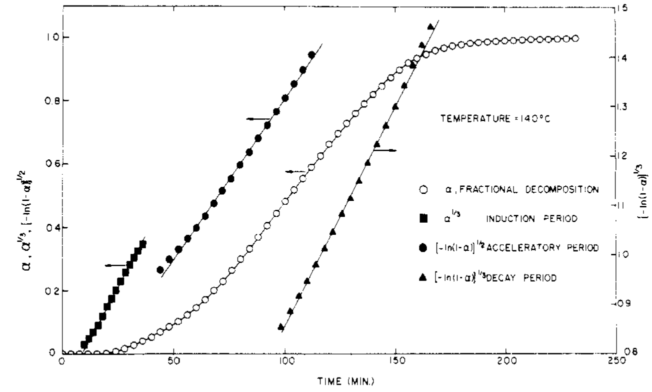

Figure 2. Fractional decomposition, $\alpha = p(t)/p_f$, vs. time and kinetic analysis ($\alpha^{1/3}$, induction period; $[-\ln(1 - \alpha)]^{1/2}$, acceleratory period; $[-\ln(1 - \alpha)]^{1/3}$, decay period, vs. time) for α-AlH_3 powder decomposed isothermally at 140 °C in vacuo.

$\alpha^{1/3}$ ($0.001 < \alpha < 0.04$) over the entire temperature range. A linear followed by an exponential α vs. t relationship was rejected because of the pronounced curvature in the plots over this region.

The respective rate constants, k_1, k_2, and k_3 for original material and k_1^*, k_2^*, and k_3^* for aged material, are tabulated in supplementary Table I. (See paragraph at end of text regarding supplementary material.) The activation energies (kJ/mol) found for aged and as-received material were (as-received material listed first) as follows: induction period, 96.1 ± 4.4, 107.0 ± 11.0; acceleratory period, 150.3 ± 10.0, 158.0 ± 12.0; decay period, 162.0 ± 11.3, 164.0 ± 9.0.

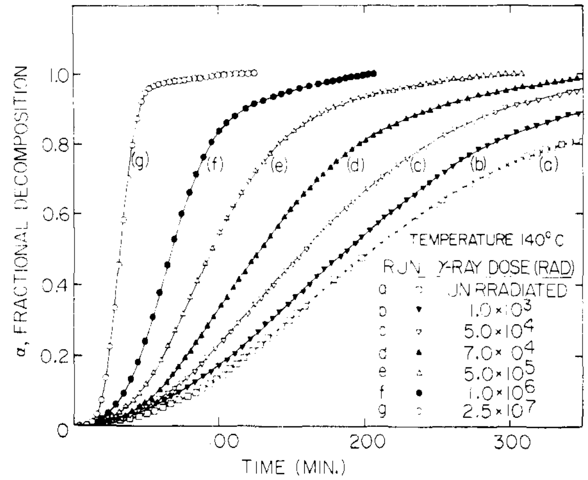

Figure 3. Effect of γ irradiation on the subsequent thermal decomposition of α-AlH$_3$ powder. This plot shows the fractional decomposition, α, vs. time for gas evolution from powder at 140 °C.

Scanning electron microscopy (SEM) affords a means of identifying the product nuclei and monitoring the progress of the reaction at various stages. We have focused attention on the intrinsic substructure of the cuboids and the thermal nucleation process. The cuboids are covered by a thin, virtually impervious layer of hydride. The formation of this "stabilizing" layer has been described in several patents.[19] This layer contains surface pits whose sides are aligned along a close-packed direction on the surface. The pit interiors are stepped and layerlike. Diffuse, colloidal-like, ellipsoidal nuclei are observed in random patches just beneath the "skin" in the early stages of the induction period. Occasionally patches of nuclei are observed before any thermal pretreatment. During the induction period the thin external surface sheath remains intact and the nuclei are observed in cracks and in subsurface regions where the sheath is thin. At very high magnifications (×36 000), later in the decomposition process, the nuclei appear as clusters of short, thick, randomly oriented needles. As the decomposition proceeds, each nucleated region does not appear to increase in thickness, but more areas of clustered nuclei appear randomly dispersed throughout the subsurface. This evidence corroborates the random nucleation and growth postulated by the decomposition kinetics. As the decomposition proceeds into the acceleratory period, bubbles (voids) appear beneath the surface, and the solid has a very mottled appearance. This subsurface activity (bubble coalescence and internal fragmentation) continues as decomposition proceeds. During the decay stage, the outer crust will fragment on occasion exposing the filamentary nature of the interior, but usually the cuboid remains intact. Briefly the SEM results show that a rapid nucleation process is occurring randomly in localized areas. The nuclei increase in number with reaction time and spread through the crystal to form voids. During this progression, blocks of partially reacted material are isolated, and the reaction is eventually confined to these blocks.

Irradiated Material. Previous work on preexposure to ionizing radiation had demonstrated that the material was sensitive to both γ-ray[6] and UV irradiation.[7] In a series of experiments using each type of radiation, the dose dependence of the radiation-induced nuclei and their sudden introduction into various stages of the decomposition was examined. These will be described below.

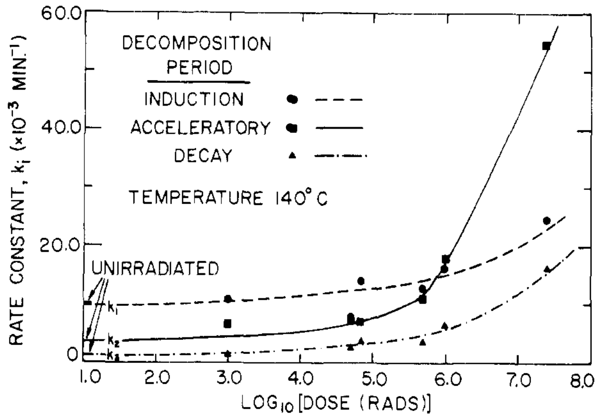

Figure 4. Effect of γ irradiation prior to decomposition on the induction-period, acceleratory-period, and decay-period rate constants (k_1, k_2, and k_3, respectively). Decomposition temperature was 140 °C.

^{60}Co γ-Rays. The effects of γ irradiation on the subsequent thermal decomposition of 3-mg samples of original powder decomposed at 140 °C is shown in Figure 3 for doses ranging from 7.0×10^4 to 2.5×10^7 rd. Irradiation darkens the powder. It also affects all three decomposition stages. The induction-period length is reduced, and both the acceleratory- and decay-period rates are increased. The irradiation α vs. time curves were subjected to the same critical kinetic analysis as the pristine powder. Equations 2 and 3 fit the irradiated data with a 0.99 correlation coefficient to the same extent as the unirradiated data over the entire dose range. The resulting rate constants are listed in Table II (supplementary material). All three constants, k_1, k_2, and k_3, increase with dose slowly up to $\sim 5.0 \times 10^5$ rd, at which point a much more rapid increase is observed (Figure 4). This marked increase in the rates coincided with the onset of hydrogen gas evolution in the encapsulated samples after irradiation; i.e., it corresponds to a dose that is producing detectable radiolysis at room temperature. After 1.0×10^7 rd the samples are black, indicative of a finely divided decomposition product.

Data from 1.0×10^6 rd preirradiated samples isothermally decomposed between 125.0 and 142.0 °C were well-fitted by the same equations as for pristine material. The resulting rate constants are tabulated in Table III (supplementary material), and the plots of ln k_{1-3} vs. $1/[T\,(\mathrm{K})]$ produced activation energies of 108.3 ± 8.0, 145.3 ± 9.2, and 162.4 ± 12.5 kJ/mol for the induction, acceleratory, and decay stages, respectively.

The shortening of the induction period by the irradiation can be attributed to the formation of additional nucleation sites. The nuclei form rapidly after heating commences as no increase in their concentration was detected before decomposition. Direct observation of an increasing number of nuclei during decomposition could not be obtained because the large number of unirradiated nuclei generated close to $t = 0$ precluded detection of any additional nuclei. However, evidence of the additional nuclei can be deduced from the results obtained when a sufficiently large quantity of new nuclei are introduced by irradiation into various stages of the decomposition. The method is described in detail in an earlier publication,[1] and the results are shown in Figure 5 (using a γ-ray dose of 1.0×10^6 rd). The arrow indicates the time at which the pristine material's decomposition was interrupted. The sample was then cooled, encapsulated, and γ-irradiated, and the decomposition was recommenced. It is important to note that a similar sequence for an unirradiated decomposition had no effect on the subsequent α vs. t curves. This result would appear

---

[19] N. E. Matzek, Dow Chemical Co., U.S. Patent 3 844 853 (1974); J. M. Self and N. E. Matzek, Dow Chemical Co., U.S. Patent 3 844 854 (1974).

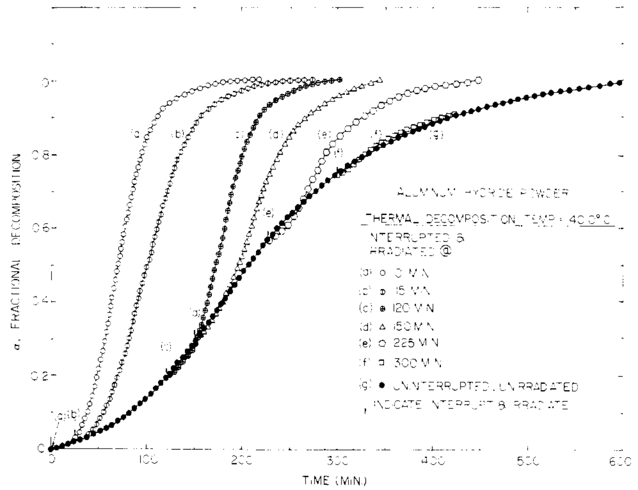

Figure 5. Data showing the effect of interrupting the decomposition of pristine material, irradiating the sample, and resuming the decomposition. The decomposition temperature was 140 °C, and the ^{60}Co γ-ray dose was 1.0 × 10^6 rd. The decomposition was interrupted (arrows) corresponding to the curves from left to right at 0, 15, 120, 150, 225, and 300 min after decomposition was started. The extreme right curve is for unirradiated material.

to eliminate the possibility that the reaction was occurring by the formation of an unstable intermediate whose lifetime was dependent on the interruption period.

The following changes occur in the decomposition curves after the interruption and irradiation event. First, the decomposition continues along the unirradiated curve for a time corresponding to a time equivalent to the induction period for the irradiated material. This elapsed time is very significant. *It shows unambiguously that an induction period exists in this material.* Second, at the end of this induction period, the decomposition rate abruptly increases and follows the shape of the uninterrupted *radiation* curve (corresponding to the preselected dose) at the corresponding α value. This effect occurs throughout the acceleratory period. When the elapsed induction-period time after interruption is such that the onset of the radiation curve occurred after the inflexion point, the subsequent irradiation decay stage is still sufficient to cause some acceleration of the reaction. Eventually, at longer times the two curves are superimposable.

This result supports the contention that irradiation produces additional nuclei and that, for a given γ dose, the radiation-produced nuclei are formed in concentrations in the bulk greater than those normally present. They grow as the decomposition proceeds and effectively "hide" or "mask" any effects due to the nuclei present in the unirradiated material. The irradiation nuclei operate throughout the acceleratory period and even, to a small extent, into the early stages of the decay period. Eventually, all of the potential sites are consumed and the effect is no longer observed. Similar effects have been found to occur on the decomposition of lithium aluminum hydride,[1] the alkaline[20] and alkaline-earth[21] permanganates, barium azide,[22] silver permanganate,[23] and ammonium perchlorate.[11]

This similarity is further strengthened by considering relationship between the induction-period length, I, with irradiation dose, Φ. It has been established that the thermal induction period of the above-mentioned materials is experimentally related to the radiation dose by eq 1. A specific combination of thermal and radiation-induced processes has been shown to produce this relationship,[13] viz., an exponential law for thermal nuclei growth and linear radiation-induced nuclei growth. The resulting equation[23] is of the form

$$I = \frac{1}{g}\left[\ln\left(\frac{N_0}{N_c} + \frac{j}{N_c}\Phi\right)\right] \quad (4)$$

where g and j are constants and N_0 and N_c are the initial and critical size of the nucleus at time $t = 0$ and $t = I$, respectively. The fit of this equation to the I and Φ data obtained at 110.6 °C is shown in Figure 6. Also shown on this plot is the theoretical equation calculated by using the linear high-dose data and the induction-period data

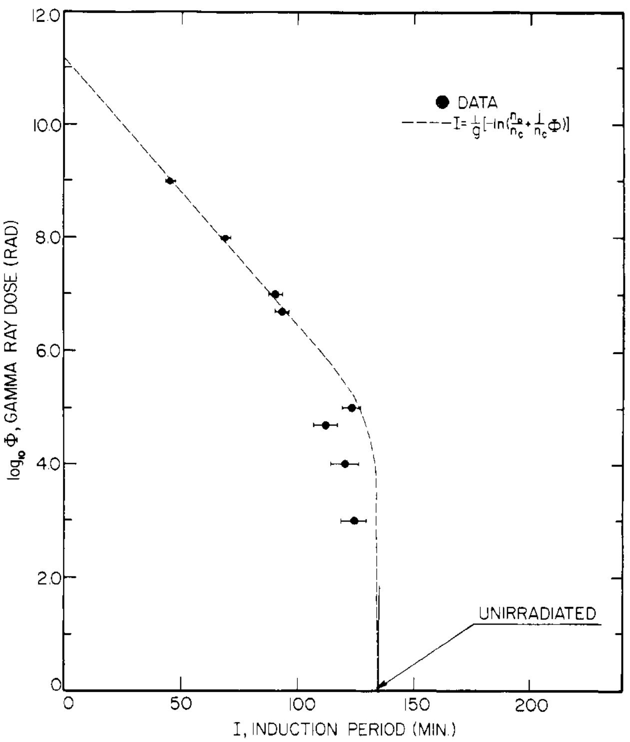

Figure 6. Induction period vs. total γ-ray dose data for α-AlH_3 powder decomposed at 110.6 °C. The dashed line was computed from eq 4 in the text by using the linear high-dose data and the length of the induction period for the unirradiated material.

TABLE IV: Ratio (N_C/N_0) of the Critical to the Initial Size, or Extent, of the Decomposition Nuclei Determined from the Radiation-Induced Decrease in the Induction Period

material	decomp temp, °C	induction period for unirradiated material, min	type of radiation	ratio
$KMnO_4$	210	47	^{60}Co γ-rays	2.0 × 10^4
	224	65	reactor	7.6 × 10^3
	224	65	^{60}Co γ-rays	1.2 × 10^3
$NaMnO_4$	140	101		1.15 × 10^2
$RbMnO_4$	230	103		3.2 × 10^2
$CsMnO_4$	240	167		1.3 × 10^4
BaN_6	110	180		4.9 × 10^8
NH_4ClO_4	227	63		6.75 × 10^4
	238	39		1.4 × 10^4
	135	19400		1.22 × 10^4
$LiAlH_4$	130	38		6.3 × 10^4
α-AlH_3	110.6	135		2.1 × 10^6

---

[20] E. G. Prout and P. J. Herley, *J. Phys. Chem.*, **66**, 961 (1962).
[21] E. G. Prout and P. J. Herley, *J. Phys. Chem.*, **65**, 208 (1961).
[22] E. G. Prout, personal communication.
[23] E. G. Prout and M. J. Sole, *J. Inorg. Nucl. Chem.*, **9**, 232 (1959).

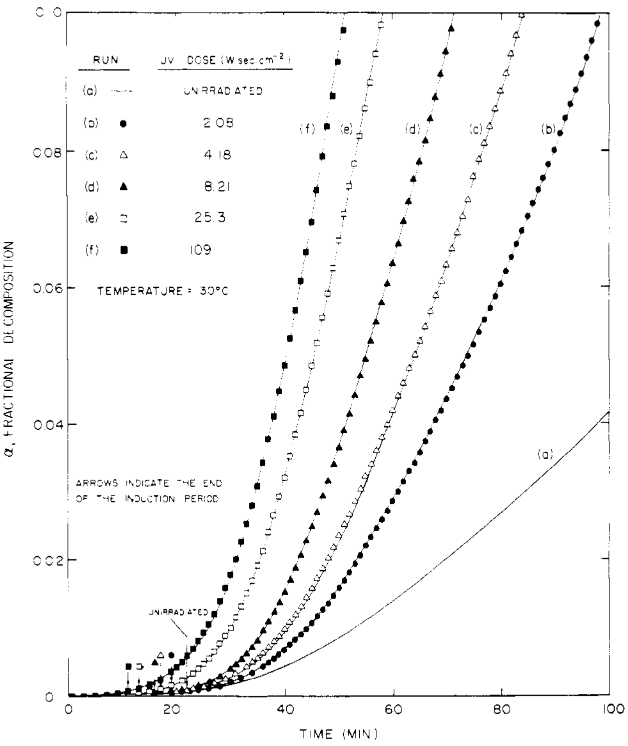

Figure 7. Details of the effect of prior UV irradiation on the thermal decomposition induction period of aged material at 130 °C. Arrows indicate the end of the induction period.

from unirradiated material. A basic tenet of eq 4 is that $N_c/N_0 \gg 1$. From the fit of eq 4 illustrated in Figure 6, a value of $N_c/N_0 = 2.1 \times 10^6$ was obtained. The results for all previously determined materials, including those for α-AlH$_3$, are tabulated in Table IV. Clearly, as predicted, N_c/N_0 is consistently greater than 1.

UV Irradiation. When a sample is UV-irradiated before thermal decomposition, the effects are similar to those found for γ-ray preirradiation; i.e., all of the periods in the subsequent thermal decomposition are reduced. The UV dose dependence of the early stages of the decomposition is shown in Figure 7 for 60-mg samples decomposed at 130 °C. Attempts to linearize the plot of induction-period length vs. log (dose) yielded a value of $N_c/N_0 \approx 5.4 \times 10^2 \pm 2.0 \times 10^2$ at 130 °C. The large standard deviations are a result of the lack of precision in accurately determining the induction-period length. The marked sensitivity of the induction period to UV irradiation is not unexpected. This period is normally associated with nucleation events on the external surface, and, as these are the areas exposed to the light, photoinduced nucleation would be favored there. However, it is also possible for photoinduced carriers to produce radiation effects at large distances from the primary event.[24] This is the likely explanation for the effects produced when the thermal decomposing sample is abruptly UV-irradiated, as illustrated in Figure 8. With a continuous UV exposure the decomposition proceeds with virtually no induction period (indicating an extremely rapid nucleation stimulus by the photons) at a rate exactly duplicating the coirradiated decomposition from $t = 0$. This accelerated coirradiated rate persists even into the last vestiges of the decay period. Several possible factors could explain this effect: either the light induces more densely packed nuclei on the subsurfaces of the interior blocks or the mobile energy carriers induced by the light generate additional decomposition sites in the interior of the blocklike product formed in the decay stage.

Discussion

The measurements described above taken in conjunction with those found in the electron microscope investigation provide considerable insight into the thermal decomposition process in α-AlH$_3$. The interior substructure of the cuboids is layerlike and is oriented along specific crystallographic planes. The crystal structure of α-AlH$_3$ is also layerlike with alternating planes of aluminum and hydrogen stacked in spirals perpendicular to the z axis of the unit cell.[15] The hydrogen and aluminum atom spirals form a completely bridged structure with a comparatively high density and a relatively high resistance to solvation. Since the Al layers contain atoms packed similar to the packing in a fccub metal, decomposition (the removal of H$_2$ from between the metal layers) can be considered as occurring by a two-dimensional lattice contraction in the x and y directions and an expansion in the z-axis direction. This lattice distortion produces decomposition nuclei which possess the characteristic elongated acicular shape.

The reproducible nature of the isothermal sigmoidal α vs. time curves can be attributed to a uniform dispersion of the predecomposition nuclei throughout the material in addition to a narrow size distribution of the cuboids themselves. The material ages slowly on standing but not rapidly enough to influence the run-to-run reproducibility. This aging effect is reflected in the occurrence of detectable decomposition nuclei prior to decomposition.

Next consider the sigmoidal nature of the α vs. t curves and their kinetic analysis. During the induction period ($0 < \alpha < 0.05$) a large number of diffuse, colloidal particles were observed to nucleate rapidly in selected subsurface areas. These areas increase in number with time, and the nuclei grow to reach their acicular, ellipsoidal shape during this period. A sharp interface between the colloidal particles and the unreacted solid is not observed; most often the particles just decrease in size below the resolution of the microscope as the interface is traversed. Both nucleation and nuclei growth are occurring simultaneously over this period, which probably accounts for the evolution of gas from time $t = 0$. It is difficult to separate the formation and growth sequences in this stage, particularly as the nucleation events occur beneath the surface layer where a distinct delineation cannot be made between surface and bulk effects. At best the induction period can be considered as a period of rapid nucleation and "slow" growth. It is a separate period with a clearly defined activation energy and is distinct from the subsequent acceleratory stage (as the radiation effects have so clearly shown). Similar nucleation events have been observed in the initial stages of the decomposition of calcium azide[25] and silver oxide.[26]

A power law fit to the data was not unexpected over this period. The 1/3 exponent of α in eq 3 predicates a multistep nucleation event. This arises from either of two postulates, each equally probable. In the first hypothesis several successive decompositions may be required to form a stable nucleus. The polymeric nature of the crystal lattice would facilitate such successive decompositions of the Al–H bonds because of the density of cross-linking in the lattice. Alternatively, decomposition may arise from the combination of two active intermediaries, each of which is formed at a constant rate. Thus H-atom generation and

---

[24] R. W. Dreyfuss and P. W. Levy, *Proc. R. Soc. London, Ser. A*, **246**, 233 (1958).

[25] F. C. Tompkins and D. A. Young, *Trans. Faraday Soc.*, **61**, 1470 (1965).

[26] P. J. Herley and E. G. Prout, *J. Am. Chem. Soc.*, **82**, 1540 (1960).

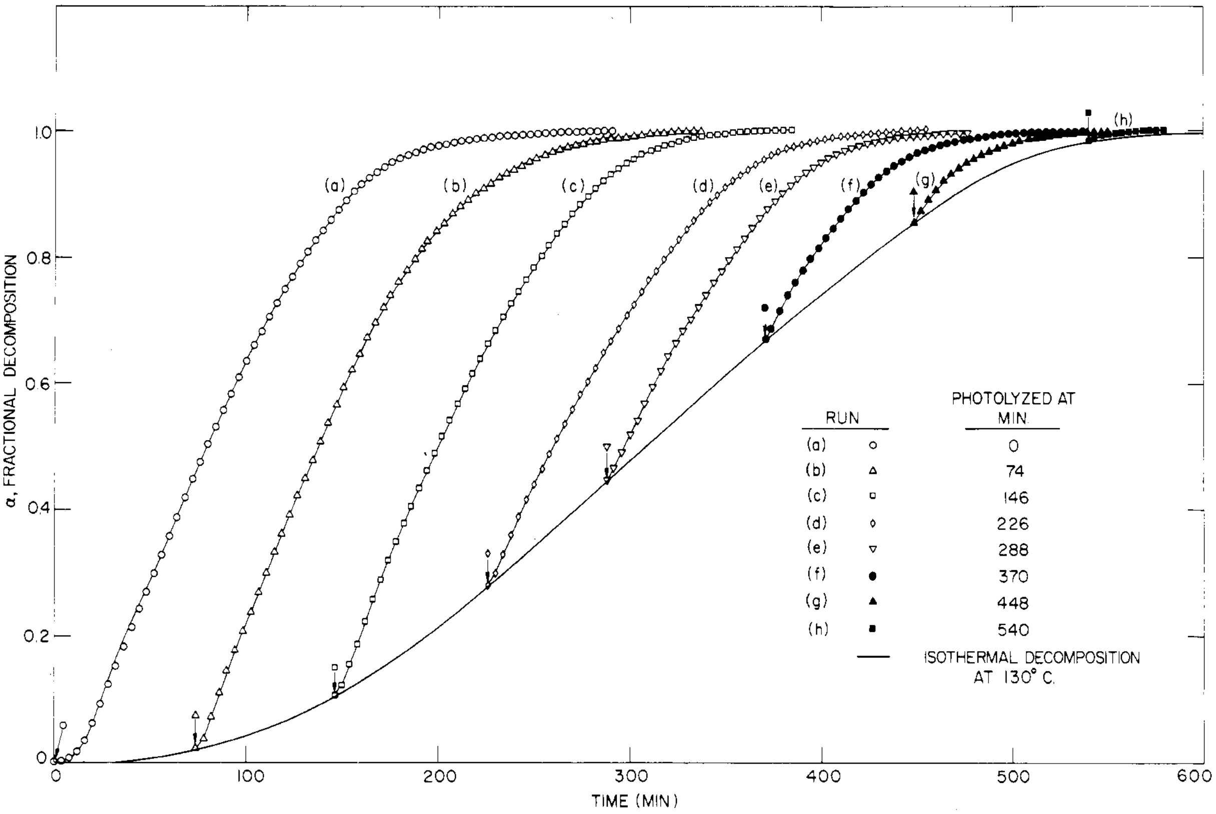

Figure 8. Data showing the effect of initiating continuous photolysis at various times during the isothermal decomposition of 60 mg of aged α-AlH_3 powder at 130 °C. The samples were exposed in each case at a constant lamp intensity, $I = 151.6$ mV cm^{-2} $\simeq$ 25% of maximum.

recombination remains an equally probable alternate.

Growth of nuclei patches randomly throughout the solid dominates the acceleratory period. A sharp interface demarcates these patches from the unreacted lattice; the decomposition kinetics are clearly different from the preceding period. The random dispersion of the nuclei and their thermal behavior (spread and overlap of the patches) is reflected in the good fit to the A–E equation. The change in exponent in the A–E equation indicates a change in the dimensionality of growth on aging. A possible explanation for this change is as follows. The predecomposition dispersed patches of nuclei will be localized initially at internal surfaces and grow randomly throughout decomposition. However, as the bulk grown nuclei concentration is increased, for example, on aging (or photolysis), a change would occur to produce a denser two-dimensional decomposition interface. The layerlike structure of the hydride would facilitate this type of interface progression. (Propagation of the reaction along the z-axis direction (along the H and Al spirals) may be rapid and not rate determining.) Enlargement of the patches would be slower in the x and y directions, and the rate of growth in these directions would be approximately equal and rate determining. This is borne out by the SEM results; the surface patches are irregularly shaped and shallow, and they cover an increasing amount of surface as the reaction proceeds. In the late stages of the acceleratory period, close to the inflexion point, bubbles (voids) appear beneath the surface leaving partially reacted material isolated between the voids. Further decomposition occurs along these mosaic block boundaries until the contracting volume mechanism is dominant.

The decay period ($0.6 < \alpha < 0.97$) is described by the A–E equation with $n = 3$. The spalling or breakup of the cuboid into small filament-covered blocks has been observed microscopically and justifies the application of the mosaic block formation mechanism. During the decay stage these blocks are transformed into Al metal via the penetration of the reaction zone through the solid. The cuboids are intact, though filamentary, at $\alpha = 1$. Apparently the coating applied to the surface hinders surface reaction, keeps the surface layer intact, but allows bulk decomposition to occur thermally and photolytically.

The exact chemical nature of this layer has not been determined, but its formation has been described in several patents.[19] Electron-induced X-ray fluorescence analysis indicates no significant increase in intensity of the Al peak on the surface or inside the bulk. (Al was the only element detected by this method.) The X-ray powder patterns of the pristine solid showed no additional lines corresponding to Al metal (though they were clearly visible in the final product). However, a few, faint lines were observed which correspond to those of Al_2O_3 powder patterns. This protective layer also contains carbonaceous material as these gases were detected in mass-spectrometric analyses of the surface layers in concentrations exceeding those of N_2 and O_2 desorbed simultaneously. The presence of this protective layer undoubtedly accounts for the marked stability of the material to water vapor (for which it was specifically designed) and for the absence of an effect with admixed powders.

The same activation energy (~160 kJ/mol) was obtained for the acceleratory and decay periods on pristine and aged material and is indicative of the same thermally assisted process occurring over both periods. The lower value (~100 kJ/mol) for the induction period reflects the enhanced reactivity of localized sites for nuclei formation. The rate constants are independent of hydrogen pressure, suggesting that the decomposition process is irreversible, independent of any gas-phase reaction.

The effects of UV and γ-ray preirradiation are also significantly interesting. The reaction is accelerated, yet the irradiated data can be analyzed by the same equations which apply to unirradiated material. In other words, the $\alpha(t)$ curves for γ- and UV-irradiated samples do not differ in any qualitative way from the unirradiated cuboids except in the value of the rate constants obtained. The activation energies are the same for all of the stages within experimental error, supporting the conclusion that the same chemical process is occurring in both preirradiated and unirradiated material. If this chemical process were directly proportional to the concentration of free carriers, e.g., electrons or holes, the ionizing radiation would produce a large nuclei concentration proportional to the radiation-induced electron and/or hole concentration. The resulting irradiated α vs. time curves would be identical with the unirradiated curves except the former would begin at shorter times; i.e., only the induction period would be shortened. Obviously this is not the case; the rate constants of all three stages exhibit a nonlinear dependence on the γ-ray dose. Furthermore, the increase in the rate constants above 1.0×10^6 rd coincides with a blackening of the sample and additional gas evolution during irradiation, i.e., the onset of radiolysis. Thus, some type of radiation decomposition mechanism is operating concurrently with the prenucleation events. Therefore, we conclude that it is unlikely that the irradiation-induced nucleation involves simple processes that are directly proportional to the free carrier concentration.

The specific type of irradiation produces differences which also need to be considered. The effects of UV light at room temperature are for the most part confined to the surface and are most pronounced over the induction period. The γ-ray radiation enhances all of the decomposition stages. The difference between the irradiation modes is most conspicuous when the interruption and irradiation experiments are examined. Unlike the γ-ray effects that are, by and large, confined to the bulk of material, UV irradation activates surface sites even over the decay stage. Additional evidence of surface nucleation induced by the light is provided by the change observed in the color of the sample surface (brown to black to silver) with increasing UV dose. The γ-ray preirradiated samples are uniformly brown before decomposition but become black throughout above doses of 1.0×10^6 rd. The acicular nuclei formed by UV irradiation are denser and thicker in the surface patches than those produced thermally.

The relationship between the radiation dose and the induction-period length, i.e., the fit of eq 1 to the data, gives rise to an apparent inconsistency. Equation 1 corresponds to a linear combination of equations representing exponential growth kinetics during heating and linear growth during irradiation. However, the present induction-period data are best fitted by the power law (eq 3) for pristine, aged, and irradiated material. The exponential law does not fit the induction-period data. This apparent inconsistency can be resolved by considering the experimental observation that nucleation occurs rapidly with "slow" growth of the nuclei in three dimensions. It can be shown that under these conditions the exponential law reduces to a power-law equation.[27]

The growth of the nuclei during irradiation is assumed to be linear. Equation 1 fits the data over several orders of magnitude, and the resulting N_c/N_0 ratio is consistent with the data for several other solids (Table IV). A comparison between the dose dependencies of the induction-period lengths indicates that α-AlH_3 is one of the materials most sensitive to ionizing radiation over this period.

Finally, these results indicate that a radiation-induced species is involved in promoting the decomposition process. Electrons, holes and/or excitons, ionization-induced species, and intrinsic defects[28] are the most likely entities to initiate the nucleation.

Acknowledgment. We thank Dr. R. Wiswall and J. Reilly, Department of Molecular Sciences, Brookhaven National Laboratory, for providing samples of the AlH_3 powder. This research was supported by the U.S. Department of Energy under Contract No. E(11-1)-2715.

Supplementary Material Available: Listings of the kinetic rate constants for original, aged, and ^{60}Co γ-ray-irradiated material (including the γ-ray dose dependence) as a function of temperature are given in supplementary Tables I–III (3 pages). Ordering information is given on any current masthead page.

---

[27] P. W. M. Jacobs and F. C. Tompkins, "Chemistry of the Solid State", W. G. Garner, Ed., Butterworths, 1955, p 193.

[28] F. C. Tompkins, "Solid State Chemistry", Vol. 4, W. B. Hannay, Ed., Plenum Press, New York, 1976, p 193.